NASA TECHNICAL NOTE

NASA TN D-6400



# EVALUATION OF HIGH-GAS-VELOCITY AND STATIC OXIDATION BEHAVIOR OF FUSED-SALT-ALUMINIDED IN 100 BETWEEN 1038° AND 1149° C

*by William A. Sanders, Charles A. Barrett, and Hubert B. Probst*

*Lewis Research Center*
*Cleveland, Ohio 44135*

NATIONAL AERONAUTICS AND SPACE ADMINISTRATION • WASHINGTON, D. C. • JULY 1971

| 1. Report No. | 2. Government Accession No. | 3. Recipient's Catalog No. |
|---|---|---|
| NASA TN D-6400 | | |

| 4. Title and Subtitle | 5. Report Date |
|---|---|
| EVALUATION OF HIGH-GAS-VELOCITY AND STATIC OXIDATION BEHAVIOR OF FUSED-SALT-ALUMINIDED IN 100 BETWEEN 1038° AND 1149° C | July 1971 |
| | 6. Performing Organization Code |
| 7. Author(s) | 8. Performing Organization Report No. |
| William A. Sanders, Charles A Barrett, and Hubert B. Probst | E-6072 |
| | 10. Work Unit No. |
| 9. Performing Organization Name and Address | 129-03 |
| Lewis Research Center<br>National Aeronautics and Space Administration<br>Cleveland, Ohio 44135 | 11. Contract or Grant No. |
| | 13. Type of Report and Period Covered |
| 12. Sponsoring Agency Name and Address | Technical Note |
| National Aeronautics and Space Administration<br>Washington, D. C. 20546 | 14. Sponsoring Agency Code |

15. Supplementary Notes

16. Abstract

Electrolytic-fused-salt-process- (EFSP-) aluminided IN 100 was cyclically oxidation tested in high-velocity combustion gas and static air from 1038° to 1149° C (1900° to 2100° F). The 0.064-mm (2.5-mil) nickel aluminide surface layer resulting from the EFSP treatment protected IN 100 for at least 400 hr at 1038° C (1900° F) and 240 hr at 1093° C (2000° F) in the high-velocity combustion gas. This protection was similar to that provided by commercial pack aluminizing. At 1149° C (2100° F) protection was less than 20 hr for the EFSP-aluminided IN 100.

| 17. Key Words (Suggested by Author(s)) | 18. Distribution Statement |
|---|---|
| Oxidation, high gas velocity; Oxidation, static; Superalloy; Aluminide protective layer; Oxidation, cyclic | Unclassified - unlimited |

| 19. Security Classif. (of this report) | 20. Security Classif. (of this page) | 21. No. of Pages | 22. Price* |
|---|---|---|---|
| Unclassified | Unclassified | 26 | $3.00 |

*For sale by the National Technical Information Service, Springfield, Virginia 22151

# EVALUATION OF HIGH-GAS-VELOCITY AND STATIC OXIDATION BEHAVIOR OF FUSED-SALT-ALUMINIDED IN 100 BETWEEN 1038° AND 1149° C

by William A. Sanders, Charles A. Barrett, and Hubert B. Probst

Lewis Research Center

## SUMMARY

Nickel-base superalloy IN 100 specimens were aluminided for oxidation protection. A surface layer of aluminum-rich nickel monoaluminide (NiAl) was formed on the IN 100 samples by an electrolytic fused-salt process (EFSP) recently commercially developed.

The IN 100 samples were tested at 1038°, 1093°, and 1149° C (1900°, 2000°, and 2100° F) in a high-gas-velocity oxidizing environment under thermal cyclic conditions, and in a static oxidizing environment at 1093° and 1149° C (2000° and 2100° F) under thermal-cycling conditions. The 0.064-millimeter (2.5-mil) layer of aluminum-rich NiAl resulting from the EFSP aluminiding treatment protected IN 100 from high-gas-velocity cyclic oxidation at 1038° C (1900° F) for at least 400 hours and at 1093° C (2000° F) for at least 240 hours. The protection was similar to that provided IN 100 aluminized in a conventional commercial pack cementation process. At 1149° C (2100° F) the EFSP-aluminided IN 100 had a life of less than 20 hours.

The EFSP-aluminided IN 100 tested in a static oxidizing environment at 1093° C (2000° F) in 2- and 20-hour-cycle tests also showed excellent oxidation resistance for at least 420 hours. At 1149° C (2100° F), static, 20-hour-cycle tests to 420 hours showed low oxidation rates for the EFSP-aluminided IN 100; however, fine spalling occurred.

From metallographic, X-ray diffraction, X-ray fluorescence, and electron microprobe analyses a model is proposed for the sequence of the oxidation of IN 100 protected with a layer of aluminum-rich NiAl provided by the EFSP metalliding process.

## INTRODUCTION

From a strength standpoint the nickel-base superalloy IN 100 is a suitable material for advanced turbine engine blading at metal temperatures near 982° C (1800° F). However, from an oxidation standpoint, IN 100 is not resistant enough for long-time service in such an application. To provide oxidation protection for superalloys, aluminide coatings are now being used, and methods for aluminide coating continue to be developed. These coatings are usually applied by the pack cementation process. Recently an electrolytic fused-salt process (EFSP) for metalliding was developed (ref. 1) for diffusing any one of a variety of metals into a metal cathode. The cathode remains completely clean since any surface oxides present are dissolved by molten salts. It was the purpose of this investigation to evaluate the oxidation protection afforded the nickel-base superalloy IN 100 by an aluminide layer resulting from the EFSP metalliding treatment.

In this application of the EFSP treatment, aluminum was diffused into IN 100 test specimens in a one-step process which resulted in the formation of an aluminum-rich nickel aluminide (NiAl) surface layer. Oxidation evaluations were performed at 1038°, 1093°, and 1149° C (1900°, 2000°, and 2100° F) for times up to 400 hours in a high-gas-velocity apparatus (ref. 2) in which the specimens are thermally cycled each hour. Specimens were also run in static-air environments under thermal-cycling conditions for times up to 420 hours. Results such as weight change, visual change, incidence of thermal fatigue cracking, degree of spalling, and results of X-ray diffraction, X-ray fluorescence, electron microprobe, and metallographic analyses were obtained.

The oxidation behavior of the EFSP-aluminided IN 100 was compared with that of bare IN 100 and IN 100 that had been pack aluminized. These comparisons were based on weight change, cracking incidence, and visual appearance.

All of the results on the EFSP-aluminided IN 100 tested in both the high-gas-velocity and the static-air environments were compared, and a detailed analysis of the results on all samples was made. This was done in order to gain some understanding of the protective mechanisms afforded the alloy by the EFSP-aluminiding treatment which provides an aluminum-rich aluminide protective layer.

## MATERIALS

The nominal composition of IN 100 is given in table I along with the compositions of gamma (nickel solid solution) and gamma prime (trinickel aluminide) phases in IN 100 which were determined by chemical separation (ref. 3).

The IN 100 test specimens were cast to shape and ground as shown in figure 1. Both the high-gas-velocity (HGV) and static samples were then commercially aluminided by

the EFSP metalliding treatment. The increases in weight on a per unit area basis due to aluminum pickup were similar for both types of samples.

The EFSP metalliding treatment resulted in the formation of NiAl surface layers which were 0.064 millimeter (2.5 mils) thick and 0.076 millimeter (3.0 mils) thick, respectively, for randomly selected sectioned and polished HGV and static samples. The thicknesses of the NiAl surface layers were measured with a microscope having a filar eyepiece. These nickel aluminide layer thicknesses were very similar to those resulting from pack aluminizing treatments.

## APPARATUS AND EXPERIMENTAL PROCEDURE

### High-Gas-Velocity Cyclic Oxidation

Figure 2 shows the high-gas-velocity cyclic oxidation apparatus used in this investigation and described in detail in reference 2. The natural-gas-fueled apparatus was operated at a combustion gas velocity of Mach 1 at the conditions given in table II. The specimens were rotated in the air-rich combustion gas stream with the tapered edges of the specimens closest to the nozzle. Rapid cooling ($55^{\circ}$ C/sec or $100^{\circ}$ F/sec) at the end of each 1-hour cycle resulted from lowering the rotating fixture into a Mach 1 cooling air blast. Temperatures were measured using a slipring thermocouple arrangement connected to a dummy specimen in the rotating fixture and were controlled by a stationary control thermocouple downstream of the test specimens. Temperature checks were made with a calibrated optical pyrometer. Specimen temperatures were maintained within $\pm 8^{\circ}$ C ($\pm 15^{\circ}$ F).

### Static-Air Oxidation

The static-air cyclic oxidation tests were performed in two ways. In the first method, the 2.54- by 5.08- by 0.254-centimeter (1- by 2- by 0.100-in.) EFSP-aluminided IN 100 specimens were supported on the edges by 99-percent-pure alumina boats. The specimens were exposed by sliding the boats into the hot zone of a horizontal, alumina tube furnace. The furnace was heated by silicon carbide resistance elements. In the second exposure method, specimens were suspended from a fixed support by a platinum/platinum-13-weight-percent-rhodium hanger wire and heated in a vertical alumina tube wire-wound resistance furnace. Cycling was effected by lowering the furnace from around the hanging sample. At the end of each cycle for both heating methods, the specimens were removed for examination and weighing. All tests were run in essentially

static air with temperatures monitored by platinum/platinum-13-weight-percent-rhodium thermocouples. Most specimens were run by a combination of both methods.

## Specimen Evaluation

Weight change. - The test specimens were weighed to the nearest 0.1 milligram prior to testing and after each test cycle for the static specimens and after 20 cycles of 1 hour for the high-velocity specimens. For comparison of static and HGV test results, the weight loss measurements in the HGV tests were divided by an area of 30 square centimeters, the estimated area of the specimen over which most of the oxidation occurred.

Visual change. - The test specimens were also examined visually under a low-power binocular microscope throughout their testing schedule, with the nature of oxide formation, color change, specimen and scale cracking, and scale spalling tendency noted, and spall collected if possible. Photographs were taken at pertinent intervals.

X-ray diffraction. - At selected intervals certain specimens were analyzed by surface X-ray diffraction with nickel-filtered, copper K-alpha radiation (40 kV, 40 mA). Any spall collected was also analyzed by a powder X-ray diffraction pattern. The phases were identified and their relative intensities noted.

X-ray fluorescence. - At intervals the static oxidation specimens were removed and analyzed by surface X-ray fluorescence. In this type of analysis, a 0.64- by 2.54-centimeter (0.25- by 1-in.) portion of the oxidized surface, or some collected and mounted spall, is exposed to tungsten or chromium radiation, and a lithium fluoride crystal detector operated at 45 kilovolts and 35 milliamperes measures the radiation. A flow of 0.28 cubic meter per hour (10 $ft^3/hr$) of helium through the specimen chamber was used. The counts were obtained for each element of interest for a given X-ray wavelength and compared to a standard of IN 100 or an aluminum planchet. The ratio of the observed counts to that of the standard was noted, and this change in ratio for a given element with the change in test conditions was a relative indicator of the compositional change for the sample.

Metallography. - Some specimens were removed from testing and sectioned for metallographic examination in order to determine how the protective layer was changing as a function of time and temperature. The test specimens were mounted perpendicularly, sectioned, and polished so that the nickel aluminide layer could be accurately observed.

The specimens were examined after various etchants had been used to bring out certain phases selectively. To bring out carbides, a solution of 10 parts potassium hydroxide, 10 parts potassium ferricyanide, and 100 parts water was used. A swab etch consisting of 30 parts acetic acid, 30 parts lactic acid, 20 parts hydrochloric acid, and 10

parts nitric acid was used to define the nickel aluminide protective layer (ref. 4). For the general structure of both the protective layer and the IN 100 substrate, an etchant consisting of 33 parts acetic acid, 33 parts glycerin, 33 parts nitric acid, and 1 part hydrofluoric acid was used.

Electron microprobe. - Selected metallographic samples were repolished and given a light vacuum deposition coating of copper to prepare the specimens for examination in the electron microprobe. Nickel, aluminum, and titanium concentration traces were made across a representative section of each specimen from the outer edge of the oxide scale through to the IN 100 substrate. Probe operating conditions were 15 kilovolts and 0.06 microampere. The probe was also operated at 10 kilovolts and 0.15 microampere to scan for secondary-electron backscatter images and X-ray fluorescence images for the elements aluminum, nickel, chromium, cobalt, titanium, and carbon. Image brightness varies directly with the amount of the element for which the scan is run. Photographs at a magnification of 667 were taken of all the images on the probe display screen. The probe concentration traces and images were used in conjunction with table I (compositions) and light photomicrographs to identify phases and to detect and interpret the changes in the test specimens.

## RESULTS AND DISCUSSION

The results of this investigation are presented in two main sections, the first dealing with the oxidation data obtained and the second concerned with the analysis of specimens.

### Oxidation Data

The results of high-gas-velocity oxidation tests for EFSP-aluminided and pack-aluminized IN 100 specimens are presented in this section along with a comparison of the behavior of EFSP-aluminided IN 100 under high-gas-velocity and static conditions.

### Weight Change and Appearance

High-gas-velocity 1038$^{o}$ C (1900$^{o}$ F) tests. - The results of weight change measurements for the 1-hour cyclic HGV oxidation tests at 1038$^{o}$ C (1900$^{o}$ F) on EFSP-aluminided IN 100 are shown in figure 3 along with data for commercially aluminized (unpublished data obtained by M. A. Gedwill of the Lewis Research Center) and bare IN 100. The EFSP nickel aluminide layer on IN 100 specimens was protective to at least 400 hours. This is concluded from the continual and regular weight increase over the

400-hour test period. Commercial pack-aluminized IN 100 exhibited similar behavior in tests stopped after 240 hours. Two of the three EFSP-aluminided IN 100 specimens showed thermal fatigue cracks by 200 hours, but the third specimen had not cracked at 400 hours when testing was stopped. No thermal fatigue cracks were noted on a commercial pack-aluminized IN 100 specimen after 240 hours. Bare IN 100 exhibited high weight loss rates from the beginning of the test, and thermal fatigue cracking was noted by 40 hours.

Photographs of EFSP-aluminided IN 100 and bare IN 100 specimens from the 1038° C (1900° F) HGV oxidation testing are presented in figure 4. The three EFSP-aluminided IN 100 specimens were uniform in appearance and showed no signs of spalling after 400 hours of exposure. Two of the three specimens had barely visible small thermal fatigue cracks at the blunt ends, but the third specimen was crack-free. Bare IN 100 developed cracks by 40 hours, and by 340 hours considerable crack growth and spalling had occurred.

High-gas-velocity 1093° C (2000° F) tests. - Figure 5 shows the results of weight change measurements for the HGV tests at 1093° C (2000° F). In these tests, the EFSP nickel aluminide layer afforded protection to IN 100 specimens for at least 120 hours. Subsequently, one of these IN 100 specimens was further tested with the EFSP nickel aluminide layer protecting it for a total of 240 hours. Total exposure for this HGV specimen was 303 hours. Protection breakdown at 240 hours was signaled by the change in slope in the continuous weight gain curve from positive to negative. At such a time, when a sustained negative slope in the plot of weight change against time is evident, it is believed that spalling is starting to occur faster than protective scale formation, and thus the ultimate destruction of the specimen is forecast. A commercial pack-aluminized IN 100 specimen (unpublished data obtained by M. A. Gedwell of the Lewis Research Center) exhibited weight change behavior similar to that of the EFSP-aluminided IN 100 and showed a thermal fatigue crack by 120 hours. Again, bare IN 100 lost weight rapidly from the start of testing and developed thermal fatigue cracks by 40 hours.

After the 1093° C (2000° F) HGV oxidation exposure EFSP-aluminided IN 100 and bare IN 100 appeared as shown in figure 6. After 303 hours the EFSP-aluminided IN 100 specimen was uniform in appearance but showed slight edge spalling. There were no thermal fatigue cracks. In contrast, bare IN 100 developed cracks at 20 hours and by 167 hours great crack growth and considerable edge spalling had occurred.

High-gas-velocity 1149° C (2100° F) tests. - At 1149° C (2100° F) the EFSP nickel aluminide layer on IN 100 was protective for less than 20 hours in HGV testing. By 20 hours the specimen had begun to lose weight rapidly, had spalled considerably, and had developed thermal fatigue cracks. No further exposures were made.

Comparison of static and high-gas-velocity 1093° C (2000° F) tests. - The results of weight change measurements for static-air oxidation test specimens of EFSP-aluminided IN 100 are shown in figure 7 along with the previously given results for the HGV

specimen exposed for 303 hours. In this figure the weight change is expressed on a per unit area basis so that the behavior of the two kinds of specimens can be compared. The comparison shows that the static-air oxidizing environment is much less severe than the HGV oxidizing environment. The oxidation rate was greater and the life shorter (protection period shorter) for the HGV specimen than for the 20-hour-cycle static specimen which was still being protected after 420 hours. (The second 20-hr-cycle static specimen was removed from testing for metallography after 120 hr.) Of course, for equivalent exposure time, the HGV test had 20 times as many cycles as did the 20-hour-cycle static-air test. And it has been shown that spalling is directly related to the number of test cycles in HGV tests (ref. 2). Also, the cooling in the HGV tests is a rapid, forced cooling, while the cooling in the static-air tests is essentially a still-air cooling. Except for an unexplained high weight gain during the first 2-hour exposure (observed on each of two specimens run together), the 2-hour-cycle static specimen which was still being protected when exposure was ended at 120 hours behaved very much like the 20-hour-cycle static specimen. This indicates that in the static-air oxidizing environment EFSP-aluminided IN 100 is insensitive to cycling in the 2- to 20-hour-cycle range.

Static 1093° and 1149° C (2000° and 2100° F) tests. - Figure 8 gives the 20-hour-cycle static-air oxidation results at 1149° C (2100° F) for two EFSP-aluminided IN 100 specimens. For comparison, also given in the figure are the 1093° C (2000° F) 20-hour-cycle static-air results. The oxidation behavior at 1149° C (2100° F) was erratic in that one specimen gained weight continually and then began to lose while the other lost at first, then gained, and then held steady. Protection began to break down beyond 120 hours and fine spalling was observed. In contrast, at the 55° C (100° F) lower temperature of 1093° C (2000° F), the 20-hour-cycle static specimen survived 420 hours with no signs of spalling.

## Analysis of Electrolytic-Fused-Salt-Process-Aluminided IN 100 Samples

Considerable pretest and post-test characterization of aluminide layers on nickel-base superalloys has been done in the past. However, the aluminide layer on IN 100 resulting from the EFSP-aluminiding treatment has not been extensively examined. It seemed then in order to characterize some of the EFSP-aluminided IN 100 specimens of this investigation. The remainder of this report is concerned with the analysis of these specimens in both the as-received and postexposure conditions. Selected specimens were subjected to X-ray diffraction, X-ray fluorescence, metallographic, and electron-microprobe analysis. These results are reviewed to arrive at a proposed model for the oxidation of EFSP-aluminided IN 100.

X-ray diffraction. - A summary of X-ray diffraction data is given in table III. It shows that at the surface of the as-EFSP-aluminided specimens only nickel aluminide was observed.

All the exposures listed indicate that the protective oxide, alpha-alumina ($\alpha$-$Al_2O_3$), formed quickly on the outer surface, that it was found for all exposures regardless of time and temperature, and that it was the only scale detected at 1038° C (1900° F). At 1093° C (2000° F) for times of 120 hours or greater, gamma prime or gamma was detected near the surface as well as small amounts of titanium dioxide. For longer times at 1093° C (2000° F) small amounts of nickel aluminum spinel ($NiAl_2O_4$) were found on static specimens, while on the high-velocity specimen at longer times, small amounts of nickel chromium spinel ($NiCr_2O_4$) were found.

At 1149° C (2100° F) alpha-alumina, gamma or gamma prime, and titanium dioxide were found as well as nickel oxide, which was also detected at longer times. Nickel-aluminum spinel was also found on the surface of the 1149° C (2100° F) test specimens. On the surface at 420 hours at 1149° C (2100° F) both light and dark areas were found, probably because of differences in spalling rates. The dark area had nickel-aluminum spinel and gamma prime as well as alpha-alumina and titanium dioxide, while the light area had nickel oxide in addition to alpha-alumina and titanium dioxide.

The appearance of titanium dioxide at the surface after some exposure suggested an outward titanium migration - possibly from a fine particulate titanium carbide zone in the nickel aluminide layer, which is described in the section High-gas-velocity 1038° C (1900° F) test. It has been suggested (ref. 5) that titanium dioxide associated with alumina permits more rapid inward diffusion of oxygen and outward diffusion of nickel and that titanium dioxide accelerates spalling.

X-ray fluorescence. - Table IV is a summary of X-ray fluorescence data for the oxidized surfaces of the static test specimens at 1093° and 1149° C (2000° and 2100° F). Also, at 1149° C (2100° F) the spall was collected in the test intervals between 120 and 260 hours and 260 and 420 hours and mounted so a surface exposure could be used. In all cases the values obtained in the table were derived by dividing the counts obtained from the test specimen by those obtained from the standard, which was always the same. For aluminum, a pure aluminum planchet was used, while for the other elements, an IN 100 standard was used. For this reason, the listed values are meaningful only where compared in the same condition (i.e., either oxidized surface or mounted collective spall) and for the same element.

These values indicate the aluminum content stayed fairly constant at the oxidized surface at 1093° C (2000° F) and dropped slightly at 420 hours. At 1149° C (2100° F) the aluminum content dropped steadily during the exposure time of 420 hours. For chromium at 1093° C (2000° F) the level stayed fairly low and relatively constant for long exposure times. At 1149° C (2100° F) chromium content was initially higher than at 1093° C

(2000° F) and rose to even higher values. Titanium content, on the other hand, started at a low value at 1093° C (2000° F) and steadily rose with time, while at 1149° C (2100° F) it started fairly high and dropped with time, probably being lost in surface spall. The values for the other elements listed in table IV do not appear to vary in a way critical to the oxidation process.

The X-ray diffraction and X-ray fluorescence results taken together show that the protective alpha-alumina formed initially on nickel aluminide, conferred oxidation protection, and was spall resistant both at 1038° and 1093° C (1900° and 2000° F). This was true even though at 1093° C (2000° F) small amounts of titanium present as titanium dioxide and gamma prime were associated with the alumina near the surface. Small amounts of nickel-aluminum spinel and nickel-chromium spinel were also found at longer times at 1093° C (2000° F). At 1149° C (2100° F), however, although the alpha-alumina still apparently formed early from the initial nickel aluminide surface layer, it tended to spall under cyclic oxidation. This spalling tendency was believed to be associated with the nickel oxide which appeared in addition to the other oxides which were noted at 1093° C (2000° F). This spalling caused disruption and loss of the protective alumina scale. Formation of fresh alumina scales then depended upon the remaining nickel aluminide layer. Continued alumina spalling and re-formation resulted in such depletion of aluminum from the nickel aluminide layer that the protection mechanism eventually broke down because of the inability to form alumina.

Metallography and electron microprobe. - The use of the electron microprobe secondary-electron backscatter images, elemental X-ray fluorescence images, and light photomicrographs is illustrated in figure 9. The specimen selected for this example had been exposed in the static-air oxidizing environment at 1093° C (2000° F) for 120 hours (20 hr cycles). A 250-magnification optical photomicrograph of the specimen etched with the general structure etchant appears in the upper left corner of figure 9. The phase identities resulted from use of the selective etchants for nickel aluminide and carbide phases and interpretation of the electron microprobe images. These images were interpreted with the aid of table I, which gives the chemical compositions of IN 100, gamma (nickel solid solution) phase in IN 100, and gamma prime (basically trinickel aluminide) phase in IN 100. For example, referring to the secondary-electron backscatter image, the band to the immediate right of the IN 100 matrix was determined to be gamma phase. This conclusion was reached by inspecting the aluminum, chromium, and cobalt fluorescence images and noting that the band was, respectively, darkest (indicating lowest aluminum content), brightest (indicating highest chromium content), and brightest (indicating highest cobalt content). The band to the right of the gamma band was determined to be gamma prime phase. Inspection of the aluminum fluorescence image showed the second band to be slightly brighter and to indicate a higher aluminum content but an aluminum content well below that of the nickel aluminide surface layer. The nickel aluminide surface layer was, of course, delineated by etching and verified by the probe images.

Finally, a carbide identified by etching was determined to be titanium carbide (TiC). For this determination, the titanium fluorescence image showed the carbide found to be very high in titanium. The titanium carbide appeared in two morphologies: as a very fine particulate form in the nickel aluminide layer, and in a massive form in the gamma and gamma prime regions.

The nickel, aluminum, and titanium microprobe traces for approximate concentrations on as-received metallographic samples were also helpful in characterizing the EFSP-aluminided IN 100. As was mentioned earlier, X-ray diffraction of the as-received static and HGV specimens showed nickel aluminide to be on the surface. That this layer extended inward for at least 0.064 millimeter (2.5 mils) was shown by the metallography and the electron microscope secondary-electron backscatter images. The microprobe concentration traces for aluminum showed that the aluminum concentration in the nickel aluminide layer on the as-received HGV sample remained nearly constant at approximately 53 atomic percent for nearly the 0.064-millimeter (2.5-mil) nickel aluminide layer thickness. However, the aluminum concentration in the nickel aluminide layer on the static as-received sample decreased continually over its 0.076-millimeter (3.0-mil) thickness from a surface high of approximately 47 atomic percent.

The titanium concentration traces made on the as-received specimens confirmed the metallographic and electron microprobe X-ray fluorescence image results. High levels of titanium were noted in the nickel aluminide layers at positions where selective etching and X-ray fluorescent images had indicated the presence of titanium carbide.

The concentration traces made on selected exposed specimens also confirmed the changes in the nickel aluminide layers observed by metallography.

Figures 10 to 12 present the microstructures of EFSP-aluminided IN 100 specimens in the as-received condition and after oxidation exposures. The microstructures were analyzed by the metallographic and electron microprobe techniques that have been described.

High-gas-velocity 1038$^{o}$ C (1900$^{o}$ F) tests: The microstructures of HGV specimens as-received and after 400 hours of cyclic exposure at 1038$^{o}$ C (1900$^{o}$ F) are shown in figure 10. In the as-received condition the IN 100 matrix was separated from the nickel aluminide protective layer by a gamma prime layer containing fingers of gamma. A zone of fine particulate titanium carbide was found in the middle of the nickel aluminide layer. The reason for the presence of this zone is not known, but such regions of fine particles which are high in titanium have also been observed in pack-aluminized IN 100 specimens (ref. 6). Zones of titanium carbide have also been observed in nickel aluminide layers on pack-aluminized IN 100 and apparently result from the stated deliberate deposition of titanium along with aluminum (ref. 5).

After 400 hours of exposure at 1038$^{o}$ C (1900$^{o}$ F) in the HGV oxidizing environment, alpha-alumina was found on the surface of the nickel aluminide layer, and gamma phase

was found in the nickel aluminide layer near the surface. No gamma prime phase could be seen associated with the gamma phase. The nickel aluminide layer had grown greatly. The portion of the nickel aluminide layer below the fine particulate titanium carbide zone contained considerable amounts of massive titanium carbide and chromium carbide particles and was separated from the coarsened IN 100 matrix by a thin band of gamma phase. The absence of any gamma prime separating gamma and nickel aluminide regions was due to the ternary equilibrium relations in the nickel-aluminum-chromium system (ref. 7). Above 1000° C (1832° F) the gamma prime field was sufficiently restricted so that beta (NiAl) may have been in equilibrium with gamma. Except for the thin gamma band, these observations are similar to those noted by the investigators in reference 4 concerning the effect of high-temperature exposure on a nickel aluminide protective layer on nickel-base superalloy MAR-M200. Other investigators (ref. 6) attribute the nickel aluminide layer growth to inward aluminum diffusion and outward nickel diffusion. It should be recalled that the nickel aluminide layer on the as-received HGV specimen of IN 100 developed by the EFSP aluminiding treatment was found to be aluminum-rich by electron microprobe analysis and therefore would have had a greater propensity to grow than a nickel aluminide layer of lower aluminum content. The investigators in reference 4 suggest that the carbides in the nickel aluminide layer result from an enrichment of titanium and chromium as a result of nickel depletion and a reaction with carbon which is diffusing outward. The coarsened IN 100 matrix was thought to reflect a decarburization by removal of carbides from grain boundaries. The growth of nickel aluminide layers on nickel-base superalloys has also been observed by the authors of reference 6, and these same authors have reported that, for comparable layer thicknesses, nickel aluminide layers with higher aluminum contents are protective longer (ref. 8).

High-gas-velocity and static 1093° C (2000° F) tests: The microstructural condition of an HGV specimen after 303 hours of oxidation exposure at 1093° C (2000° F) is shown in figure 11. Oxidation resulted in a surface layer of gamma phase above the nickel aluminide layer and separated from the nickel aluminide layer by a discontinuous layer of gamma prime phase. Patches of alpha-alumina were found on the gamma phase surface. Again, the nickel aluminide layer portion below the fine particulate titanium carbide zone had grown, but the nickel aluminide portion above the fine particulate titanium carbide zone had been almost completely consumed in this case. The expanded nickel aluminide layer contained large quantities of gamma prime at the nickel aluminide grain boundaries. The coarsened IN 100 matrix was separated from the expanded nickel aluminide layer by a gamma phase containing large gamma prime and titanium carbide particles.

The microstructures of static specimens as received and after 120 hours (2-hr cycles), 120 hours (20-hr cycles), and 420 hours (20-hr cycles) are shown in figure 11. In the as-received condition the IN 100 matrix was separated from the nickel aluminide protective layer by a thin gamma phase zone. No gamma prime layer was observed. As

for the HGV as-received specimen, the nickel aluminide layer contained a middle zone of fine particulate titanium carbide. However, the nickel aluminide portion below the titanium carbide zone in the static as-received specimen contained large titanium carbide and chromium carbide particles, while none were noted in the HGV as-received specimen. It should be recalled that the electron microprobe concentration traces for the as-received static specimen showed a lower aluminum concentration at the surface of the nickel aluminide protective layer than the aluminum concentration at the surface of the nickel aluminide protective layer of the HGV as-received specimen. Also, the aluminum concentration in the nickel aluminide protective layer dropped gradually from the surface inward to its boundary with the gamma zone. On the other hand, the nickel aluminide layer on the as-received HGV specimen maintained the high aluminum content it displayed at its surface almost its entire measured thickness. These facts suggest that the static as-received specimen received a somewhat different treatment which resulted in a greater inward diffusion of aluminum for the static specimen than for the HGV specimen.

The 2- and 20-hour-cycle static specimens exposed for 120 hours at 1093$^{o}$ C (2000$^{o}$ F) were microstructurally similar in several respects, as noted in figure 11. Both had gamma prime phase at the nickel aluminide layer surface and within the nickel aluminide. Both had the fine particulate titanium carbide zone and nickel aluminide layer thicknesses similar to that of the as-received static specimen. Also, in both specimens, gamma phase layers separated very similar IN 100 matrices from the material above. However, the 20-hour-cycle sample had well developed layers of gamma and gamma prime phase, while in the 2-hour-cycle specimen the demarcation between the two layers was not so clear. Also, the gamma layer of the 2-hour-cycle specimen contained a second phase precipitate. This was no doubt gamma prime phase, probably coarsened by the repeated solution and reprecipitation occurring during each cycle. The lack of such precipitation in the 20-hour-cycle specimen probably reflected the lesser number of cycles to which this specimen was subjected.

Another difference was the presence of a gamma phase layer with some alpha-alumina patches above the nickel aluminide layer of the 20-hour-cycle specimen; this was lacking in the 2-hour-cycle specimen, where the 10 times greater cycling frequency would likely have resulted in more spalling.

The microstructure of the 420-hour, 20-hour-cycle static specimen was similar to that of the 120-hour-exposure specimen but showed that more gamma prime phase was present in the then somewhat expanded nickel aluminide layer. No gamma phase was found at the nickel aluminide surface. Chromium carbide was found in the lower portion of the nickel aluminide layer in association with gamma prime phase particles. The IN 100 matrix had coarsened in comparison to the 120-hour condition, and titanium carbide and chromium carbide particles were noted in the matrix grain boundaries.

Static 1149° C (2100° F) tests: Microstructures for static specimens exposed for 120 and 420 hours (both 20-hr cycles) at 1149° C (2100° F) are given in figure 12. The 120-hour condition was very similar to that of the 120-hour, 20-hour-cycle, 1093° C (2000° F) static specimen except that the surface gamma phase layer was somewhat heavier. One interesting observation was that the titanium carbide zone in the nickel aluminide layer formerly referred to as "fine particulate" appeared to have collected into a dense, thin layer. By 420 hours, at 1149° C (2100° F) diffusion and oxidation had consumed the entire nickel aluminide layer and left a thin gamma phase zone with alpha-alumina patches at the surface above a gamma prime phase region which was formerly nickel aluminide. The titanium carbide zone was again present. A gamma phase layer separated the gamma prime phase region from the coarsened IN 100 matrix.

An indicator of aluminum depletion from nickel aluminide other than the appearance of the lower aluminum content gamma prime and gamma phases was the appearance of well defined striations in the nickel aluminide grains. In this work, such striations were observed in a few nickel aluminide grains (faintly discernible in figs. 11 and 12). These striations have been observed in bulk nickel aluminide and interpreted by Rosen and Goebel (ref. 9) as being due to a martensitic reaction in a nickel-rich nickel aluminide. More recently, Smialek (ref. 10) has observed these striations in the microstructures of nickel aluminide coatings on nickel-base superalloys IN 100 and B 1900 which had been exposed to high-temperature oxidation.

## PROPOSED OXIDATION MODEL

From the observations made as a result of the oxidation tests conducted on EFSP-aluminided IN 100 an oxidation model is proposed which can be outlined as follows:

(1) Alpha-alumina forms a protective outer layer over nickel aluminide.

(2) Alpha-alumina continues to form to replenish spall losses as long as nickel aluminide is available.

(3) The nickel aluminide layer grows by inward aluminum diffusion from an aluminum-rich nickel aluminide.

(4) Titanium dioxide ($TiO_2$) begins to appear at the surface and accelerates oxygen diffusion and oxide spalling.

(5) After some exposure at 1093° C (2000° F) aluminum depletion reaches a point where less protective spinels, nickel aluminate (static) or nickel chromate (HGV), form. Nickel oxide (NiO) appears with nickel aluminate in static tests at 1149° C (2100° F).

(6) The formation of NiO is associated with the spalling of the remaining protective alpha-alumina layer.

This model agrees with the general observations which have been made by others (refs. 4 to 6 and 8). We suggest that the origin of the titanium for the $TiO_2$ formation is the fine particulate titanium carbide zone near the midpoint of the nickel aluminide layer of the as-received EFSP-aluminided IN 100 specimens.

## CONCLUSIONS

High-gas-velocity and static oxidation behavior of fused-salt-aluminided IN 100 between 1038° and 1149° C (1900° and 2100° F) was studied, and the following conclusions were drawn:

1. Electrolytic-fused-salt-process- (EFSP-) aluminided IN 100 is equivalent in high-gas-velocity cyclic oxidation resistance to pack-aluminized IN 100 at 1038° and 1093° C (1900° and 2000° F). The 0.064-millimeter (2.5-mil) nickel aluminide surface layer resulting from the EFSP treatment protects IN 100 for at least 400 hours at 1038° C (1900° F) and 240 hours at 1093° C (2000° F) in a high-velocity combustion gas stream.

2. The mechanisms by which the EFSP nickel aluminide layer protects a nickel-base alloy and eventually degrades in protection ability appear to be identical to those believed to be operable for nickel aluminide layers resulting from pack aluminizing.

3. An EFSP nickel aluminide layer on IN 100 offers considerably more protection in a static-gas environment than in one of high-velocity gas. At 1093° C (2000° F) usable life in a static environment (420 hr) is at least twice as great as that in a high-velocity gas stream. The difference becomes even greater at 1149° C (2100° F).

Lewis Research Center,
National Aeronautics and Space Administration,
Cleveland, Ohio, April 14, 1971,
129-03.

## REFERENCES

1. Cook, Newell C.: Metalliding. Scientific Am., vol. 221, no. 2, Aug. 1969, pp. 38-46.

2. Johnston, James R.; and Ashbrook, Richard L.: Oxidation and Thermal Fatigue Cracking of Nickel- and Cobalt-Base Alloys in a High Velocity Gas Stream. NASA TN D-5376, 1969.

3. Kriege, Owen H.; and Baris, J. M.: The Chemical Partitioning of Elements in Gamma Prime Separated from Precipitation-Hardened, High-Temperature Nickel-Base Alloys. Trans. ASM, vol. 62, no. 1, Mar. 1969, pp. 195-200.

4. Goward, G. W.; Boone, D. H.; and Giggins, C. S.: Formation and Degradation Mechanisms of Aluminide Coatings on Nickel-Base Superalloys. Trans. ASM, vol. 60, no. 2, June 1967, pp. 228-241.

5. Redden, T. K.: Ni-Al Coating-Base Metal Interactions in Several Nickel-Base Alloys. Trans. AIME, vol. 242, no. 8, Aug. 1968, pp. 1695-1702.

6. Moore, V. S.; Bretnall, W. D.; and Stetson, A. R.: Evaluation of Coatings for Cobalt- and Nickel-Base Superalloys. Vol. 1, Rep. RDR-1474-2, Solar Div. International Harvester Co. (NASA CR-72359), Jan. 31, 1969.

7. Taylor, A.; and Floyd, R. W.: The Constitution of Nickel-Rich Alloys of the Nickel-Chromium-Aluminum System. J. Inst. Metals. vol. 81, pt. 9, May 1953, pp. 451-464.

8. Moore, V. S.; Bretnall, W. D.; and Stetson, A. R.: Evaluation of Coatings for Cobalt- and Nickel-Base Superalloys. Vol. 2, Rep. RDR-1474-3, Solar Div. International Harvester Co. (NASA CR-72714), July 1970.

9. Rosen, S.; and Goebel, J. A.: The Crystal Structure of Nickel-Rich NiAl and Martensitic NiAl. Trans. AIME, vol. 242, no. 4, Apr. 1968, pp. 722-724.

10. Smialek, James L.: Martensite in NiAl Oxidation-Resistant Coatings. Metallurg. Trans., vol. 2, no. 4, Apr. 1971.

11. Anon.: High Temperature High Strength Nickel Base Alloys. International Nickel Co., Inc., rev. ed. 1964.

TABLE I. - COMPOSITIONS OF IN 100 (NOMINAL), GAMMA, AND GAMMA PRIME PHASES IN IN 100

[Data obtained by chemical separation.]

| Material | Nickel | Chromium | Cobalt | Aluminum | Molybdenum | Titanium | Vanadium | Zirconium | Carbon | Boron |
|---|---|---|---|---|---|---|---|---|---|---|
| | Concentration, wt. % | | | | | | | | | |
| IN 100[a] | 60 | 10 | 15 | 5.5 | 3 | 4.7 | 1 | 0.6 | 0.18 | 0.014 |
| Gamma in IN 100[b] | 46 | 22 | 24 | 2.3 | 5.3 | .4 | --- | --- | ---- | ----- |
| Gamma prime in IN 100[b] | 68.6 | 3.3 | 10.7 | 7.1 | 1.3 | 7.7 | 1.3 | --- | ---- | ----- |

[a]Ref. 11.
[b]Ref. 3.

TABLE II. - CONDITIONS FOR HIGH-GAS-VELOCITY OXIDATION TESTS

| | |
|---|---|
| Maximum specimen temperature, $^{o}C$ ($^{o}F$) | 1038, 1093, or 1149 (1900, 2000, or 2100) |
| Burner gas temperature, $^{o}C$ ($^{o}F$) | 1427 to 1538 (2600 to 2800) |
| Gas velocity | Mach 1 |
| Burner pressure, $mN/m^2$ (psia) | 0.023 (33) |
| Specimen rotational speed, rpm | 900 |
| Burner airflow, kg/sec (lb/sec) | 0.41 to 0.45 (0.9 to 1.0) |
| Cooling airflow, kg/sec (lb/sec) | 0.23 (0.5) |
| Air-fuel ratio | 20 to 30 |
| Burner nozzle diameter, cm (in.) | 5.1 (2.0) |
| Specimen test cycle | 1 hr at max temperature, 3 min cooling to room temperature |

TABLE III. - X-RAY DIFFRACTION OF AS-RECEIVED AND OXIDIZED EFSP-ALUMINIDED IN 100

[Intensities taken from outer surface except where noted.]

| Temperature | | Specimen[a] | Exposure time, hr | Cycle length, hr | Phase | | | | Spinel[b] | | |
|---|---|---|---|---|---|---|---|---|---|---|---|
| °C | °F | | | | NiAl (lattice parameter, m; Å) | Gamma or gamma prime | $\alpha$-$Al_2O_3$ | $TiO_2$ | NiO | $NiAl_2O_4$ (lattice parameter, m; Å) | $NiCr_2O_4$ (lattice parameter, m; Å) |
| | | | | | X-ray diffraction relative intensity[c] | | | | | | |
| ---- | ---- | SA-7 | As EFSP metallided | | S ($(2.882\pm0.001)\times10^{-10}$; 2.882±0.001) | -- | -- | -- | -- | ---------- | ---------- |
| | | HGV-2, -7 | As EFSP metallided | | S ($(2.873\pm0.003)\times10^{-10}$; 2.873±0.003) | -- | -- | -- | -- | ---------- | ---------- |
| 1038 | 1900 | HGV-8 | 400 | 1 | -- | -- | S | -- | -- | ---------- | ---------- |
| 1093 | 2000 | SA-7 | 2 | 2 | -- | -- | S | -- | -- | ---------- | ---------- |
| | | HGV-5 | 50 | 1 | -- | -- | S | -- | -- | ---------- | ---------- |
| | | SA-2 | 120 | 20 | -- | S | S | W | -- | ---------- | ---------- |
| | | SA-3 | 120 | 2 | -- | S | S | W | -- | ---------- | ---------- |
| | | HGV-5 | 120 | 1 | -- | S | S | -- | -- | ---------- | ---------- |
| | | HGV-5 | 210 | 1 | -- | M | M | -- | -- | ---------- | ---------- |
| | | SA-9 | 260 | 20 | -- | S | M | M | -- | VW ($8.12\times10^{-10}$; 8.12) | ---------- |
| | | HGV-5 | 260 | 1 | W | S | S | M | -- | ---------- | VW ($8.31\times10^{-10}$; 8.31) |
| | | HGV-5 | 303 | 1 | -- | S | S | -- | -- | ---------- | W ($8.31\times10^{-10}$; 8.31) |
| | | SA-9 | 420 | 20 | -- | M | S | M | -- | W ($8.09\times10^{-10}$; 8.09) | ---------- |
| 1149 | 2100 | SA-1 | 120 | 20 | -- | S | S | M | T | W ($8.07\times10^{-10}$; 8.07) | ---------- |
| | | SA-5 | 120 | | -- | S | S | S | -- | ---------- | ---------- |
| | | SA-5 | 260 | | -- | S | S | S | M | M ($8.10\times10^{-10}$; 8.10) | ---------- |
| | | SA-5 (spall) | 120 to 260 | | -- | -- | S | M | M | ---------- | M ($8.20\times10^{-10}$; 8.20) |
| | | SA-5 (dark area) | 420 | | -- | S | S | M | -- | M ($8.10\times10^{-10}$; 8.10) | ---------- |
| | | SA-5 (light area) | 420 | | -- | -- | S | W | M | ---------- | ---------- |
| | | SA-5 (spall) | 260 to 420 | | -- | -- | S | S | M | M ($8.10\times10^{-10}$; 8.10) | ---------- |

[a]Static air, SA; high gas velocity, HGV.

[b]Lattice parameters for pure spinels: $NiAl_2O_4$, $8.05\times10^{-10}$ m (8.05 Å); $NiCr_2O_4$, $8.32\times10^{-10}$ m (8.32 Å).

[c]Strong, S; medium, M; weak, W; very weak, VW; trace, T.

TABLE IV. - X-RAY FLUORESCENCE ANALYSIS RESULTS FOR EFSP-ALUMINIDED IN 100 STATIC-AIR OXIDATION SPECIMENS

| Area analyzed | Temperature | | Specimen | Exposure time, hr | Cycle length, hr | Aluminum | Chromium | Titanium | Cobalt | Vanadium | Iron | Molybdenum | Nickel |
|---|---|---|---|---|---|---|---|---|---|---|---|---|---|
| | °C | °F | | | | I/I standard[a] | | | | | | | |
| Oxidized surface | 1093 | 2000 | SA-7 | 2 | 2 | 0.21 | 0.30 | 0.04 | 0.85 | 0.12 | ---- | 0.26 | 1.1 |
| | | | SA-3 | 120 | 2 | .21 | .48 | .65 | .84 | .47 | 1.0 | .38 | 1.0 |
| | | | SA-2 | 120 | 20 | .21 | .67 | .97 | .77 | .54 | .92 | .66 | .72 |
| | | | SA-9 | 260 | 20 | .20 | ---- | 2.1 | ---- | .80 | ---- | ---- | ---- |
| | | | SA-9 | 420 | 20 | .17 | .51 | 2.5 | .68 | .60 | .89 | .65 | .70 |
| | 1149 | 2100 | SA-1 | 120 | 20 | 0.23 | 0.82 | 1.3 | 0.88 | 0.73 | 0.85 | 0.79 | 0.79 |
| | | | SA-5 | 260 | 20 | .14 | .85 | .90 | .89 | .67 | .89 | .71 | .82 |
| | | | SA-5 (dark area) | 420 | 20 | .11 | 2.5 | .71 | .89 | .58 | .91 | .81 | .81 |
| | | | SA-5 (light area) | 420 | 20 | .08 | 1.8 | .66 | .98 | .67 | .95 | .77 | .88 |
| Collected spall | 1149 | 2100 | SA-5 | 120 to 260 | 20 | 0.12 | 0.04 | 1.3 | 0.03 | 0.24 | ---- | 0.01 | 0.02 |
| | | | SA-5 | 260 to 420 | 20 | .05 | .27 | .84 | .16 | .22 | ---- | .01 | .13 |

[a]Ratio of observed counts to that of standard; for aluminum, standard was aluminum planchet, for other elements standard was IN 100 coupon.

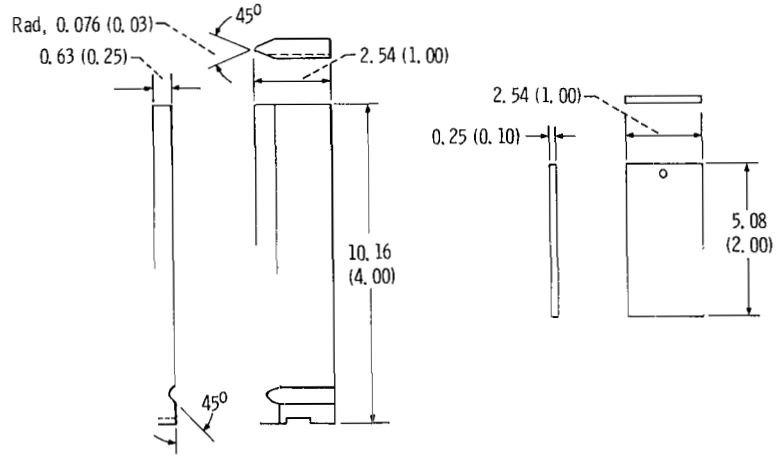


(a) High-gas-velocity oxidation specimen. (b) Static oxidation specimen.

Figure 1. - Oxidation test specimens. (Dimensions in cm (in.).)

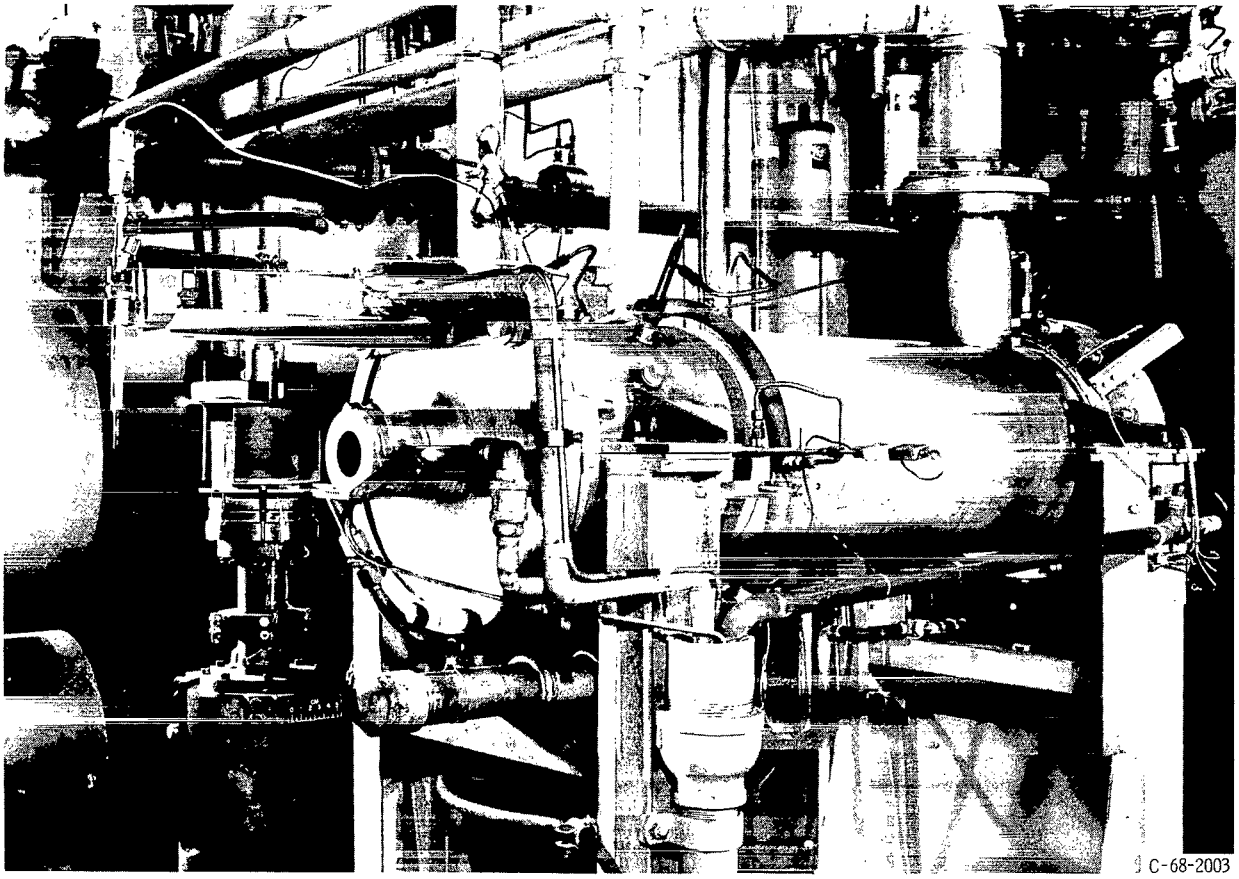


(a) Overall view.

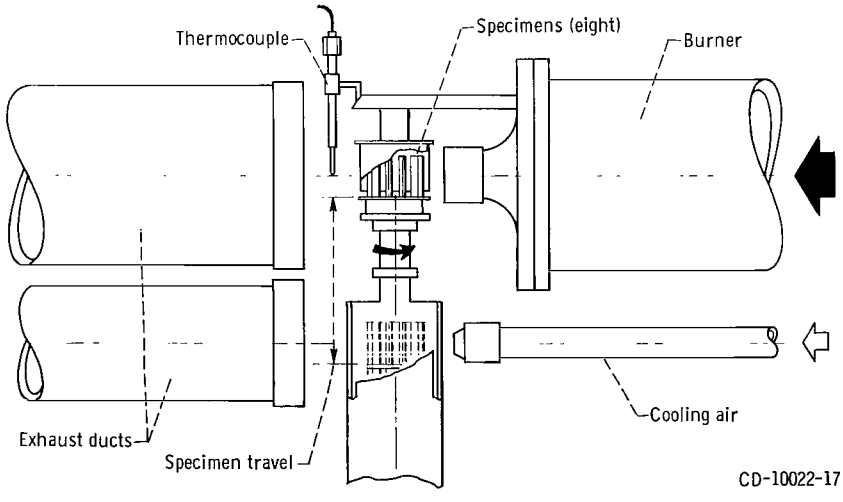


(b) Schematic diagram.

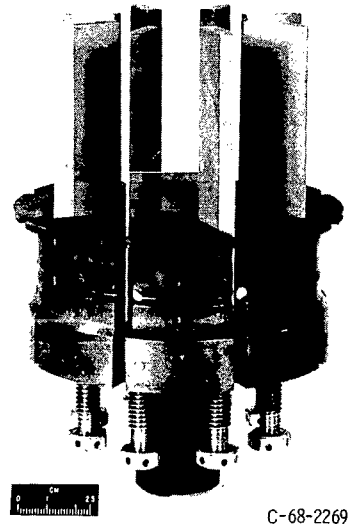


(c) Specimen holder assembly.

Figure 2. - High-gas-velocity oxidation apparatus.

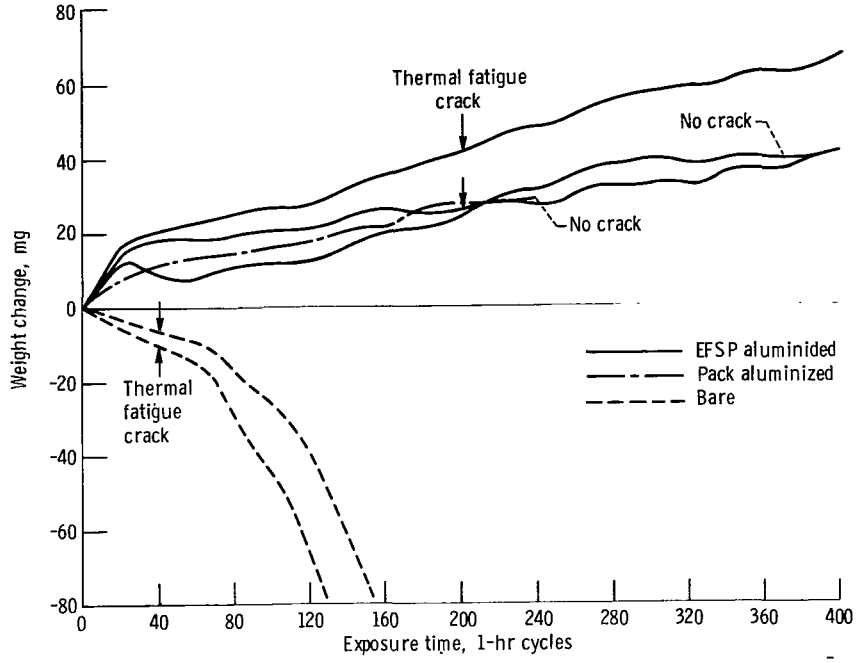


Figure 3. - High-gas-velocity cyclic oxidation of EFSP-aluminided, pack-aluminized, and bare IN 100 at 1038° C (1900° F).

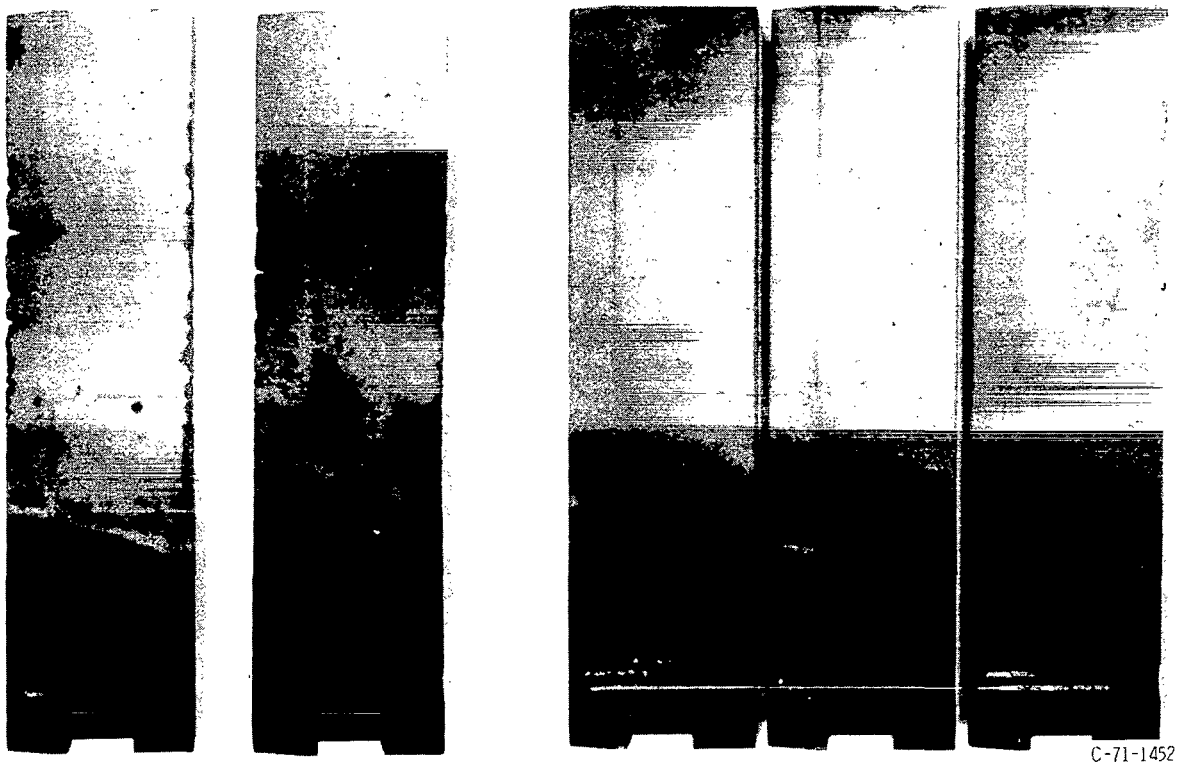


Figure 4. - Bare and EFSP-aluminided IN 100 specimens after high-gas-velocity cyclic oxidation at 1038 C (1900 ' F).

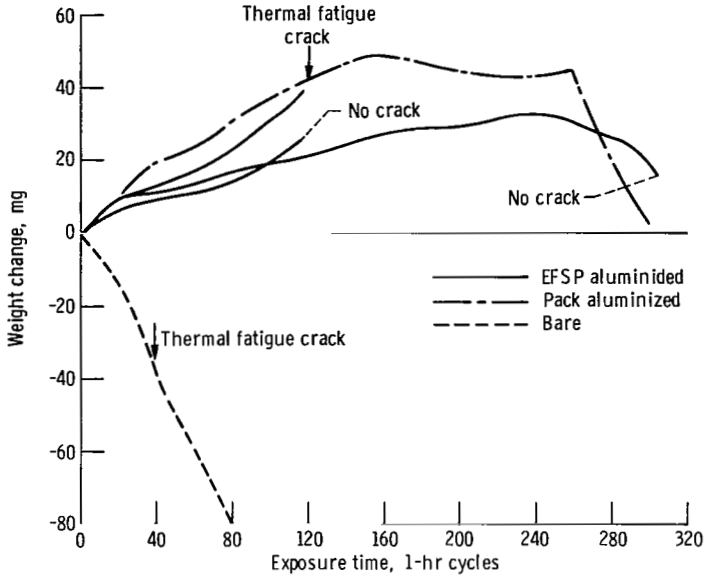


Figure 5. - High-gas-velocity cyclic oxidation of EFSP-aluminided, pack-aluminized, and bare IN 100 at 1093° C (2000° F).

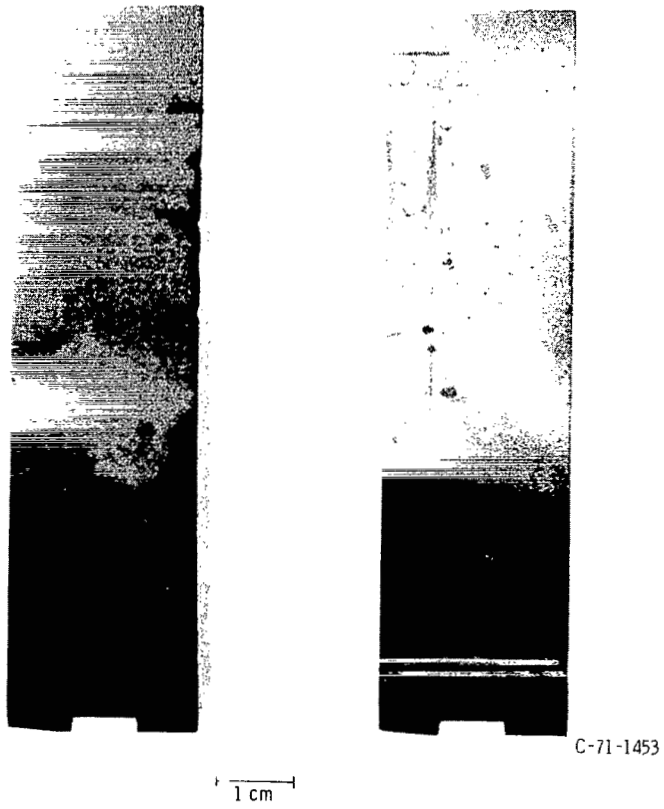


Bare IN 100; 167-hr exposure EFSP-aluminided IN 100; 303-hr exposure

Figure 6. - Bare and EFSP-aluminided IN 100 specimens after high-gas-velocity cyclic oxidation at 1093° C (2000° F).

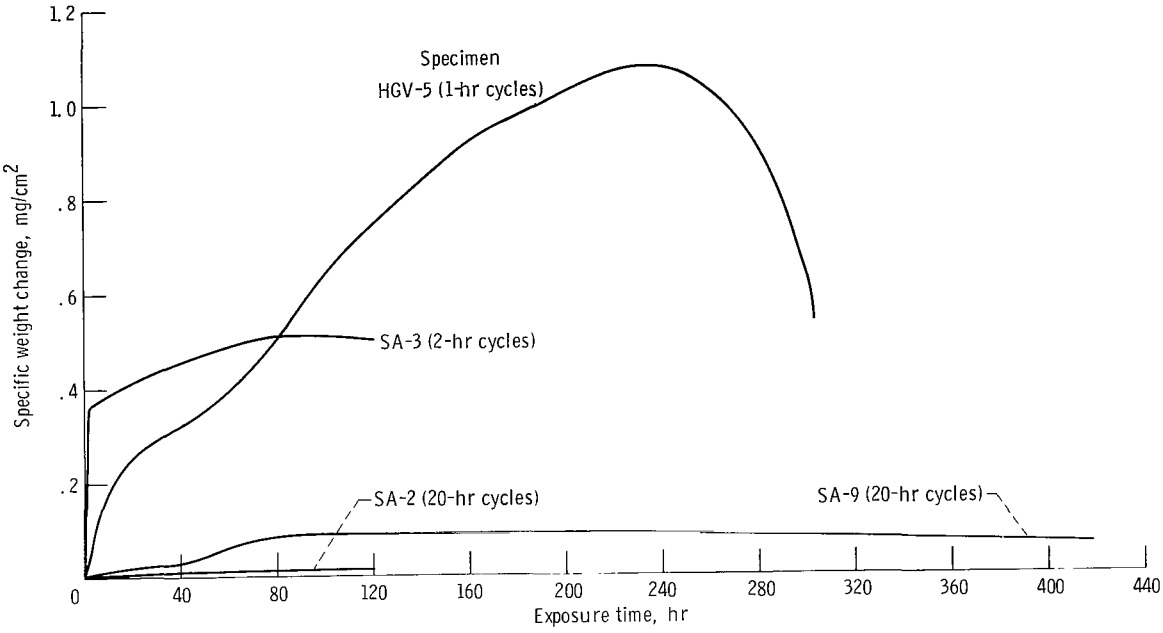


Figure 7. - Static and high-gas-velocity oxidation of EFSP-aluminided IN 100 at 1093° C (2000° F).

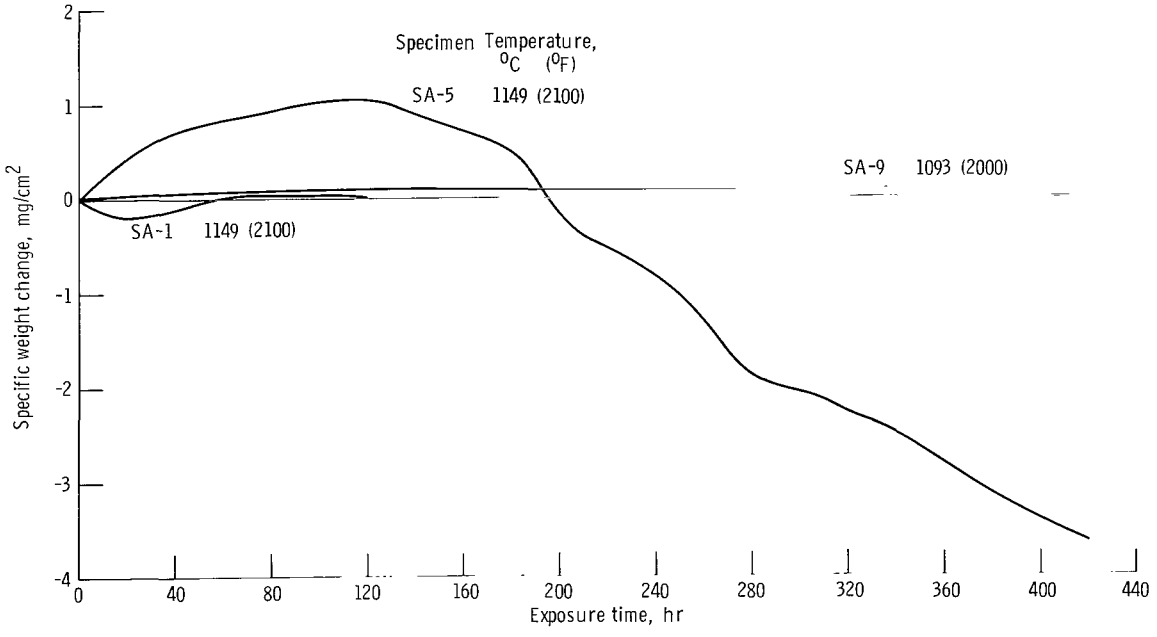


Figure 8. - Static oxidation of EFSP-aluminided IN 100 at 1093° C (2000° F) and 1149° C (2100° F) (20-hr cycles).

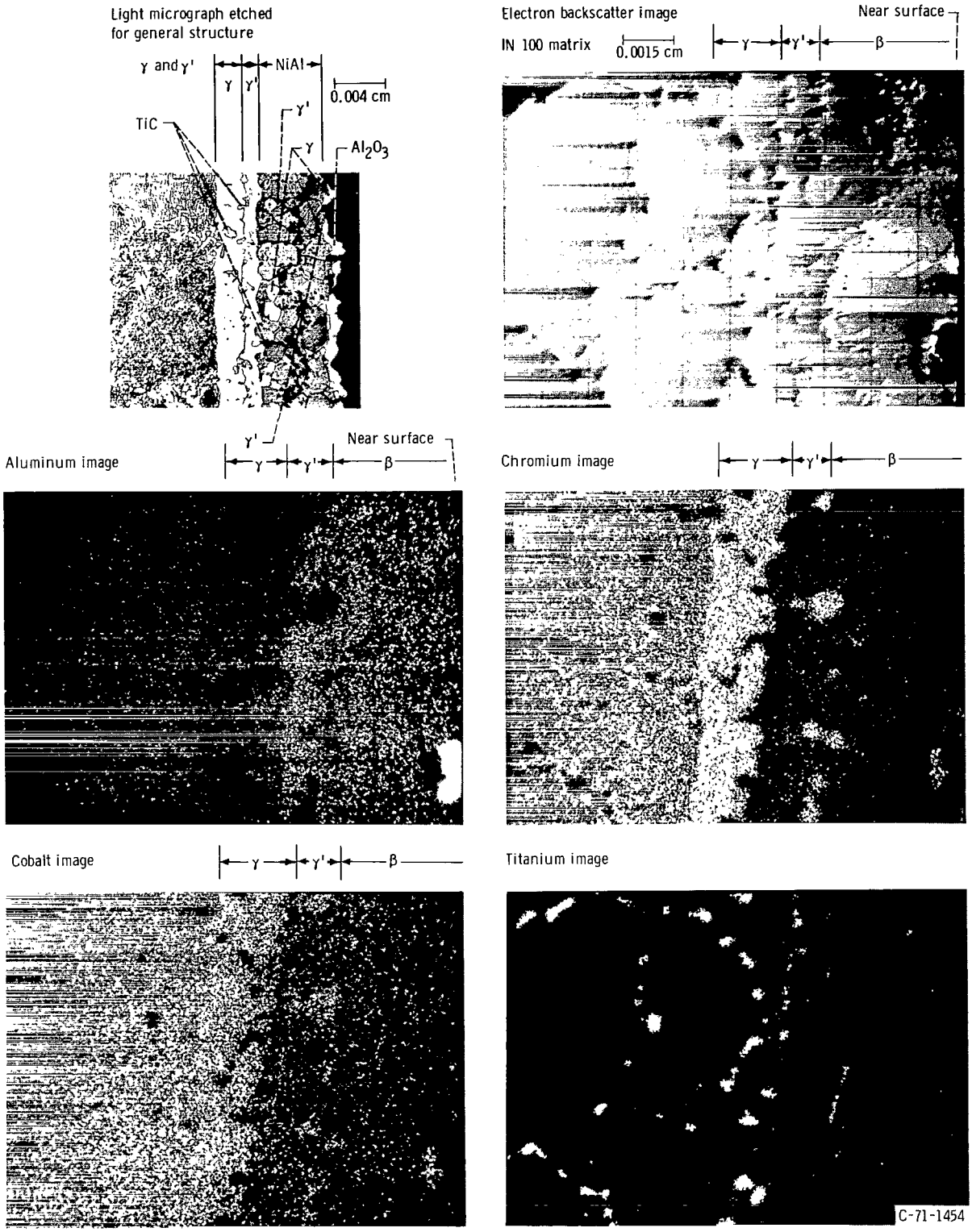


Figure 9. - Phase identification by microprobe using backscatter electron and X-ray raster micrograph images. EFSP-aluminided IN-100 static-air specimen oxidized at 1093° C (2000° F) for 120 hours in 20-hour cycles.

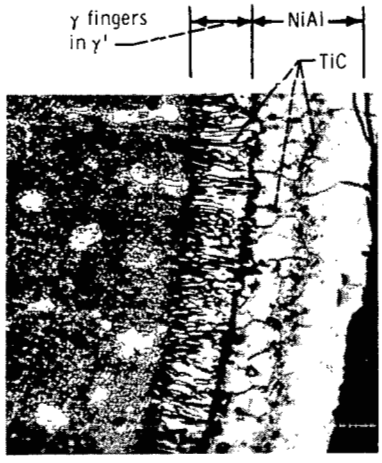


Specimen HGV-8; as received; NiAl thickness, 0.064 mm (2.5 mils)

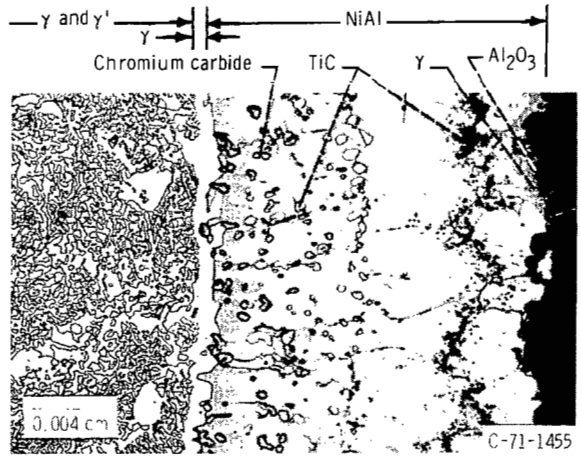


Specimen HGV-8; after 400 1-hr cycles

Figure 10. - Microstructures for high-gas-velocity EFSP-aluminided IN 100 specimens, as received and after 1038° C (1900° F) oxidation.

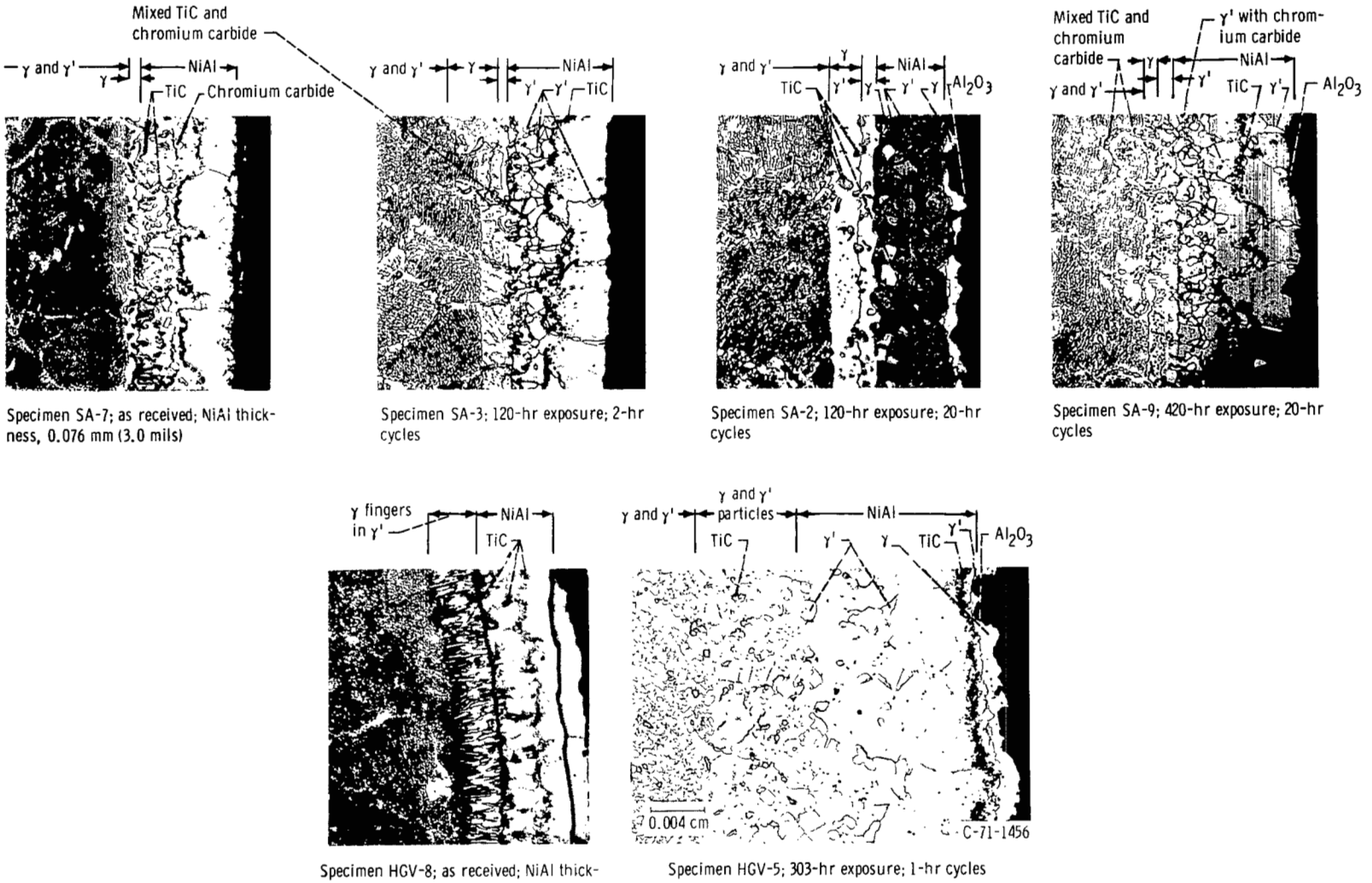


Specimen SA-7; as received; NiAl thickness, 0.076 mm (3.0 mils)

Specimen SA-3; 120-hr exposure; 2-hr cycles

Specimen SA-2; 120-hr exposure; 20-hr cycles

Specimen SA-9; 420-hr exposure; 20-hr cycles

Specimen HGV-8; as received; NiAl thickness, 0.064 mm (2.5 mils)

Specimen HGV-5; 303-hr exposure; 1-hr cycles

Figure 11. - Microstructures for static-air and high-gas-velocity EFSP-aluminized IN 100 specimens, as received and after 1093° C (2000° F) oxidation.

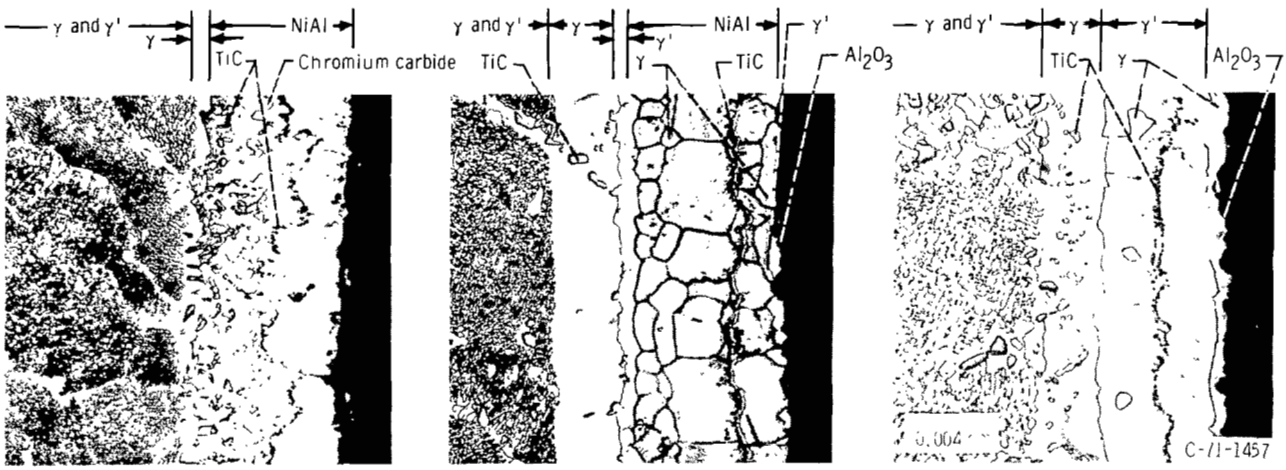


Specimen SA-7; as received; NiAl thickness 0.076 mm (3.0 mils)

Specimen SA-1; 120-hr exposure; 20-hr cycles

Specimen SA-5; 420-hr exposure; 20-hr cycles

Figure 12. - Microstructures for static-air EFS[illegible]-aluminided IN 100 specimens, as received and after 1149° C (2100° F) oxidation.

002 001 C1 U 17 710701 S00903DS
DEPT OF THE AIR FORCE
WEAPONS LABORATORY /WLOL/
ATTN: E LOU BOWMAN, CHIEF TECH LIBRARY
KIRTLAND AFB NM 87117



*"The aeronautical and space activities of the United States shall be conducted so as to contribute . . . to the expansion of human knowledge of phenomena in the atmosphere and space. The Administration shall provide for the widest practicable and appropriate dissemination of information concerning its activities and the results thereof."*

—NATIONAL AERONAUTICS AND SPACE ACT OF 1958

# NASA SCIENTIFIC AND TECHNICAL PUBLICATIONS

TECHNICAL REPORTS: Scientific and technical information considered important, complete, and a lasting contribution to existing knowledge.

TECHNICAL NOTES: Information less broad in scope but nevertheless of importance as a contribution to existing knowledge.

TECHNICAL MEMORANDUMS: Information receiving limited distribution because of preliminary data, security classification, or other reasons.

CONTRACTOR REPORTS: Scientific and technical information generated under a NASA contract or grant and considered an important contribution to existing knowledge.

TECHNICAL TRANSLATIONS: Information published in a foreign language considered to merit NASA distribution in English.

SPECIAL PUBLICATIONS: Information derived from or of value to NASA activities. Publications include conference proceedings, monographs, data compilations, handbooks, sourcebooks, and special bibliographies.

TECHNOLOGY UTILIZATION PUBLICATIONS: Information on technology used by NASA that may be of particular interest in commercial and other non-aerospace applications. Publications include Tech Briefs, Technology Utilization Reports and Technology Surveys.

*Details on the availability of these publications may be obtained from:*

**SCIENTIFIC AND TECHNICAL INFORMATION OFFICE**

**NATIONAL AERONAUTICS AND SPACE ADMINISTRATION**

**Washington, D.C. 20546**